Receptor trafficking controls weak signal delivery: a strategy used by c-Met for STAT3 nuclear accumulation

Stéphanie Kermorgant[1] and Peter J. Parker[2]

[1]Department of Tumour Biology, Cancer Research UK Clinical Centre, Bart's and the London Queen Mary's School of Medicine and Dentistry, London EC1M 6BQ, England, UK
[2]Protein Phosphorylation Laboratory, Cancer Research UK London Research Institute, London WC2A 3PX, England, UK, and Division of Cancer Studies, King's College School of Medicine, Guy's Hospital, London SE1 9RT, England, UK

C-Met, the receptor of hepatocyte growth factor (HGF), through overexpression or mutation, is a major protooncogene that provides an attractive molecular target for cancer therapy. HGF/c-Met–induced tumorigenesis is dependent, in part, on the transcription factor and oncogene signal transducer and activator of transcription 3 (STAT3), which is believed to be activated by the receptor at the plasma membrane and then to travel to the nucleus where it acts. We demonstrate that although the robust signal to STAT3 elicited from the cytokine oncostatin-M does indeed support this mechanism of STAT3 action, for the weaker STAT3 signal emanating from c-Met, the activated receptor itself needs to be delivered to a perinuclear endosomal compartment to sustain phosphorylated STAT3 in the nucleus. This is signal specific because c-Met–induced extracellular signal-regulated kinase nuclear accumulation does not require receptor trafficking to the perinuclear compartment. This response is triggered from peripheral endosomes. Thus, control of growth factor receptor traffic determines the nature of the signal output, providing novel opportunities for intervention.

Introduction

C-Met overexpression correlates closely with metastatic tendency and poor prognosis (Trusolino and Comoglio, 2002; Birchmeier et al., 2003). In addition, several germline and somatic missense mutations of c-Met, which lead to increased tyrosine kinase activity, have been reported in various tumors (Graveel et al., 2005). Hence, c-Met is an attractive molecular target for cancer therapy (Christensen et al., 2005).

The oncogene signal transducer and activator of transcription 3 (STAT3) acts downstream of c-Met to control c-Met–dependent tubulogenesis (Boccaccio et al., 1998), wound healing (Sano et al., 1999), invasion (Cramer et al., 2005), anchorage-independent growth, and tumorigenic growth in nude mice (Zhang et al., 2002). HGF was reported to stimulate STAT3 recruitment to c-Met at the plasma membrane, its phosphorylation on tyrosine 705, nuclear translocation, and binding to the specific promoter element Sis-inducible element (Boccaccio et al., 1998). Because the biological effect of STAT transcriptional activity requires entry into the nucleus, cytoplasmic-nuclear translocation of STAT proteins is crucial (Reich and Liu, 2006). Although endosomal transport has recently been proposed as a possible requirement (Bild et al., 2002; Howe, 2005; Shah et al., 2006), the current favored model of STAT3 response to stimuli is free cytosolic diffusion from the plasma membrane to the nucleus.

Increasing awareness of the importance of compartmental signaling of cell surface receptors (Miaczynska et al., 2004; Kholodenko, 2006; Polo and Di Fiore, 2006) and downstream signaling and effectors, as recently shown for Akt pathway (Schenck et al., 2008), questions whether a diffusion model is correct. It has been shown previously that c-Met signals emanate not only from the plasma membrane but also from endosomal compartments (Kermorgant et al., 2004; Kermorgant and Parker, 2005). It is

Correspondence to Peter J. Parker: peter.parker@cancer.org.uk

Abbreviations used in this paper: CHC, clathrin heavy chain; EEA1, early endosome autoantigen 1; ERK, extracellular signal-regulated kinase; HGF, hepatocyte growth factor; STAT3, signal transducer and activator of transcription 3.

The online version of this article contains supplemental material.

The Rockefeller University Press $30.00
J. Cell Biol. Vol. 182 No. 5 855–863
www.jcb.org/cgi/doi/10.1083/jcb.200806076

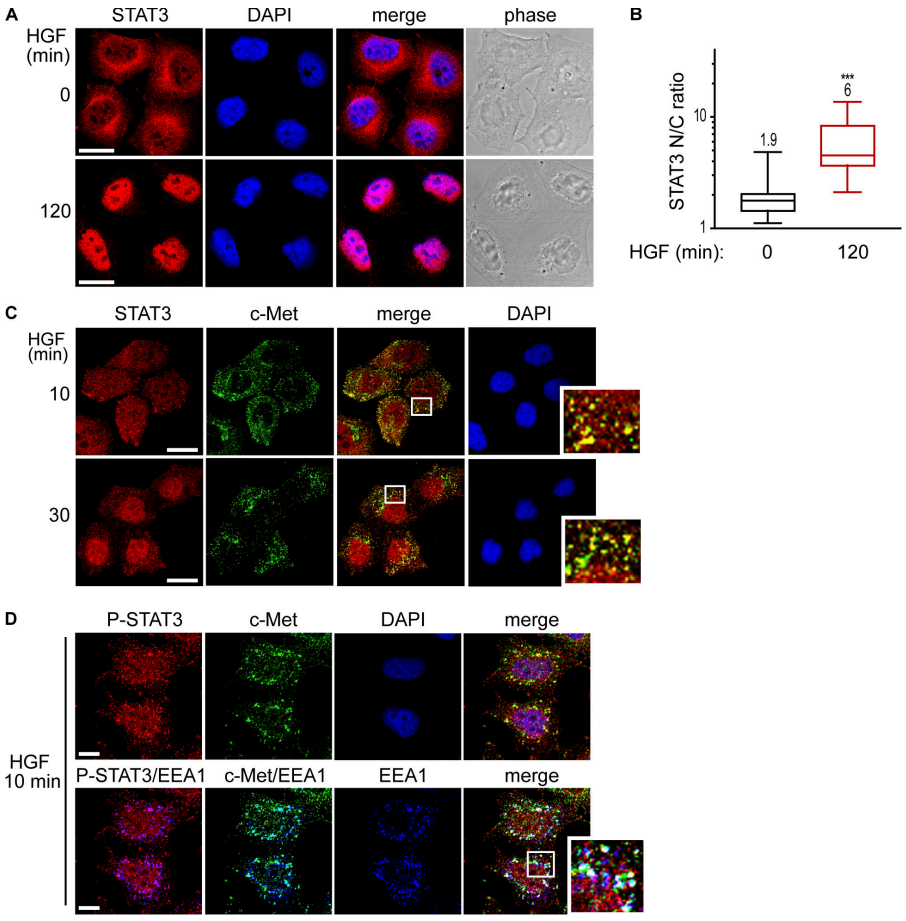

Figure 1. **C-Met and STAT3 colocalize on endosomes.** (A) Confocal sections of HeLa cells stimulated with HGF for 0 or 120 min and stained for STAT3 and DAPI. Bars, 20 µm. (B) Quantitation of STAT3 nuclear-cytoplasmic ratios (STAT3 N/C ratio) at 0 or 120 min of HGF stimulation. Statistical analyses of five independent experiments are presented as box and whiskers plots (see Statistical analysis of confocal images). The mean values are on top of each box. ***, $P < 0.0001$. (C) Cells stimulated with HGF for 10 or 30 min were stained for STAT3, c-Met, and DAPI. Confocal sections are shown. Bars, 20 µm. (D) Cells stimulated with HGF for 10 min were stained for P-STAT3 (Y705), c-Met, DAPI, and EEA1. Confocal sections are shown. White boxes define the enlarged areas shown at the right. Bars, 10 µm.

demonstrated here that STAT3 activation and nuclear accumulation in response to HGF requires nuclear-proximal activated c-Met.

Results and discussion

C-Met and STAT3 colocalize on endosomes before STAT3 nuclear accumulation

In HeLa cell cultures, STAT3 is localized in the cytoplasm (Fig. 1 A and Fig. S1 A, available at http://www.jcb.org/cgi/content/full/jcb.200806076/DC1) but can be present to a variable extent in the nucleus (Fig. S1 A, top). This distribution is likely the consequence of continuous shuttling under basal conditions (Pranada et al., 2004; Liu et al., 2005). Stimulation with hepatocyte growth factor (HGF) for 120 min leads to a significant increase in nuclear accumulation of STAT3 (Fig. 1, A and B; and Fig. S1 A). The STAT3 nuclear accumulation on HGF stimulation correlates with a strong nuclear signal for STAT3 phosphorylated on tyrosine 705 (Fig. S1 B). These results indicate that, according to current models, nonphosphorylated STAT3 undergoes nuclear-cytoplasm shuttling under basal conditions and that HGF stimulates phosphorylated STAT3 nuclear accumulation.

C-Met rapidly internalizes through the clathrin pathway and then further traffics from endosomes to a nondegradative perinuclear endosomal compartment (Kermorgant et al., 2003). During its intracellular trafficking, c-Met colocalizes with pan-STAT3 and phospho-STAT3 on early endosome autoantigen 1 (EEA1)–positive endosomes (Fig. 1, C and D), indicating that STAT3 can access the active, trafficking receptor.

STAT3 and extracellular signal-regulated kinase (ERK) 1/2 nuclear accumulation upon HGF stimulation is dependent on c-Met endocytosis

Perturbation of the endocytic machinery either by knocking down clathrin heavy chain (CHC) or by expressing myc-AP180C or by treating cells with concanavalin A have been reported previously to block c-Met internalization (Fig. S1, D and E; and Fig. S2 A; Kermorgant et al., 2004). Blockade is also observed with dynasore, a recently described cell-permeable inhibitor of dynamin (Fig. 2, C and D; Macia et al., 2006). Confirmation of receptor endocytosis impairment in cells treated by dynasore and/or transfected by myc-AP180C was performed by measuring cellular uptake of fluorescently tagged transferrin and HGF (Fig. S1, C–F).

It was detected that HGF/c-Met–dependent STAT3 and also ERK1/2 nuclear accumulation are impaired significantly when c-Met endocytosis is inhibited (Fig. 2, A–H). However, receptor traffic is not a universal requirement because dynasore or expression of myc-AP180C does not impair the cytokine oncostatin M–induced STAT3 nuclear accumulation (Fig. 2, C, E, and F). Thus, although the oncostatin M receptor has been reported to become internalized (Heinrich et al., 2003), STAT3 nuclear delivery, upon stimulation with this cytokine, appears to

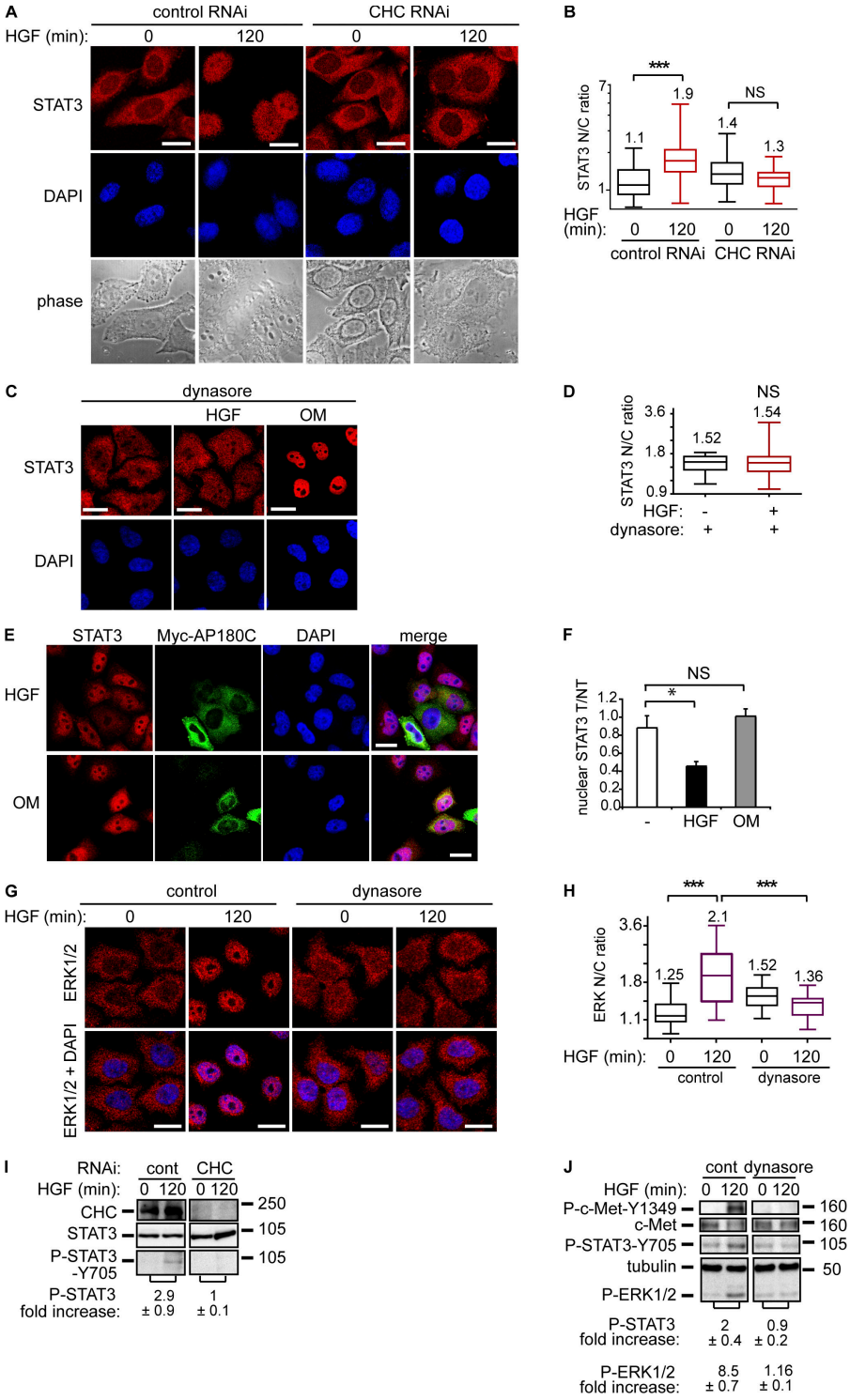

Figure 2. **STAT3 and ERK1/2 nuclear accumulation is dependent on c-Met endocytosis.** In A and B, HeLa cells transfected with control or CHC RNAi were treated by HGF for 0 or 120 min. (A) Confocal projections of cells stained for STAT3 and DAPI. Bars, 20 µm. (B) Quantitation of STAT3 nuclear-cytoplasmic ratios (STAT3 N/C ratio). ***, $P < 0.0001$. (C) Cells incubated in 80 µM dynasore were not stimulated or stimulated with HGF for 120 min or oncostatin M for 30 min. Confocal sections of cells stained for STAT3 and DAPI. Bars, 20 µm. (D) Quantitation of STAT3 nuclear-cytoplasmic ratios. (E) Confocal projections of five Z sections of cells transfected (T) or not (NT) with myc-AP180C and stained with STAT3, Myc, and DAPI after 120 min of stimulation with HGF or oncostatin M. Bars, 20 µm. (F) Quantitation of STAT3 nuclear intensity in Myc-AP180C T versus NT. The graphs show the nuclear STAT3 accumulation expressed as a ratio (T/NT) for myc-AP180C transfected versus nontransfected cells. The columns are mean values and the error bars are SD. An unpaired *t* test was performed. *, $P < 0.01$. (G) Cells were stimulated with HGF for 0 and 120 min in the absence or presence of 80 µM dynasore. Confocal sections of cells stained for ERK1/2 and DAPI are shown. Bars, 20 µm. (H) Quantitation of ERK1/2 nuclear-cytoplasmic ratios. ***, $P < 0.0001$. (I and J). Cells were treated by HGF for 0 or 120 min. Western blots for CHC, phosphorylated STAT3 (Y705), pan-STAT3, phosphorylated c-Met (tyrosine 1349), pan–c-Met and phosphorylated ERK1/2. The numbers represent fold increase of P-STAT3/STAT3 or P-STAT3/tubulin and P-ERK/tubulin ratios between HGF for 120 and 0 min obtained by densitometry in three independent experiments. (I) Cells were transfected with control or CHC RNAi. (J) Cells were treated or not by 80 µM dynasore. Molecular masses are shown in kD.

be independent of the endocytic machinery. This is consistent with the previous findings (Heinrich et al., 2003). The distinctive responses to HGF and oncostatin M indicate that STAT3 delivery to the nucleus can operate through distinct mechanisms in the same cell. STAT3 Y705 phosphorylation was reported not to play a role in STAT3 cytoplasmic-nuclear shuttling under basal conditions (Pranada et al., 2004; Liu et al., 2005), although it was reported to control STAT3 nuclear accumulation upon cytokine or growth factor stimulation (Liu et al., 2005). Consistent with this and with our immunofluorescence data (Fig. S1 B), it was observed by Western blot that, in parallel to the nuclear accumulation, STAT3 was phosphorylated on Y705 after 2 h (Fig. 2 I), which is indicative of a role for tyrosine phosphorylation in nuclear accumulation. In addition, when the endocytic machinery was perturbed through CHC knockdown, dynasore, or concanavalin A treatment, STAT3 Y705 and ERK1/2 phosphorylation were inhibited (Fig. 2, I and J; and Fig. S2 C), thus mirroring the loss of nuclear STAT3 and ERK1/2. C-Met

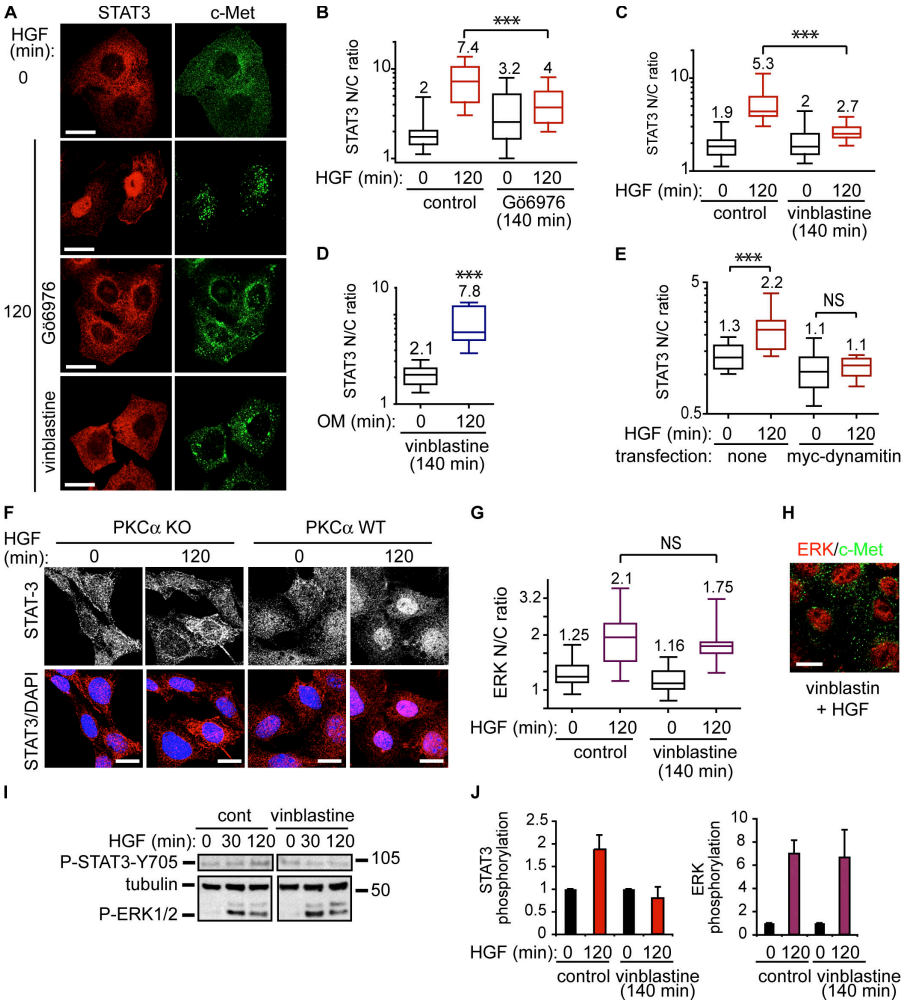

Figure 3. **STAT3, but not ERK1/2, nuclear accumulation is promoted by c-Met microtubule-dependent traffic.** (A) HeLa cells stimulated with HGF for 0 or 120 min alone or in the presence of 1 μM Gö6976 or 1 μM vinblastine were stained for STAT3 and c-Met. Confocal sections are shown. Bars, 20 μm. (B and C) Quantitation of STAT3 nuclear-cytoplasmic ratios (STAT3 N/C ratio). ***, $P < 0.0001$. (D) Quantitation of STAT3 nuclear-cytoplasmic ratios under oncostatin M stimulation for 0 and 120 min in presence of 1 μM vinblastine. ***, $P < 0.0001$ (pictures not shown). (E) Cells were transfected with myc-dynamitin and stained with STAT3, Myc, and DAPI after 120 min of stimulation with HGF. The plot represents the quantitation of STAT3 nuclear-cytoplasmic ratios in nontransfected and transfected cells. ***, $P < 0.0001$ (Fig. S2 E [pictures], available at http://www.jcb.org/cgi/content/full/jcb.200806076/DC1). (F) Confocal projections of PKCα knockout or wild-type mouse embryo fibroblasts, stained for STAT3 and DAPI. Bars, 20 μm. (G) Quantitation of ERK1/2 nuclear-cytoplasmic ratios in cells stimulated with HGF for 0 or 120 min in the absence or presence of 1 μM vinblastine. (H) Confocal section of ERK1/2 nuclear localization and endosomal c-Met in cells stimulated with HGF and vinblastine for 120 min. Bar, 20 μm. (I) Cells were stimulated with HGF for 0, 30, or 120 min in the absence or presence of 1 μM vinblastine. Western blots for phosphorylated STAT3 (Y705), tubulin, and phosphorylated ERK1/2. Molecular masses are shown in kD. (J) Densitometric analysis of I. The bars represent fold increase of P-STAT3/tubulin and P-ERK/tubulin ratios between HGF for 120 and 0 min obtained by densitometry in three independent experiments. Error bars represent SEM.

phosphorylation was also reduced under these conditions (Fig. 2 J and Fig. S2 C; Kermorgant et al., 2004). These results indicate that to sustain their phosphorylation, STAT3 and ERK1/2 require c-Met endocytosis as well as the maintainance of active c-Met. This response to the blockade of c-Met endocytosis was specific to the Y705 input to STAT3 because the serine 727 phosphorylation induced by HGF was unaffected (unpublished data).

STAT3, but not ERK1/2, nuclear accumulation upon HGF stimulation is dependent on c-Met trafficking to a perinuclear localization

It was shown previously that c-Met traffics from a peripheral endosomal compartment to a perinuclear endosomal compartment along the microtubule network and that this is facilitated by PKCα catalytic activity (Kermorgant et al., 2003). PKCα inhibition by Gö6976 (but not inhibition after c-Met traffic; see Fig. 4, A and B), or microtubule disruption by vinblastine, led to a reduction of HGF/c-Met–dependent STAT3 nuclear accumulation (Fig. 3, A–C; and Fig. S2 D). This paralleled the perturbation in c-Met traffic, which showed a decrease in perinuclear endosomal c-Met and sustained peripheral endosomal c-Met (Fig. 3 A, right). In contrast to HGF, vinblastine did not block oncostatin M–dependent STAT3 nuclear accumulation (Fig. 3 D). Overexpression of p50/dynamitin, which was previously shown to block dynein-dependent endosomal movements along the microtubules in HeLa cells (Burkhardt et al., 1997), also impaired HGF-dependent STAT3 nuclear accumulation (Fig. 3 E and Fig. S2 E). Similar results were obtained in HeLa cells knocked down for PKCα (Fig. S2, F–H) and in PKCα knockout mouse fibroblasts (Fig. 3 F). It can be concluded that c-Met directional trafficking from the peripheral endosomal compartment toward the perinuclear endosomal compartment is required for HGF/c-Met to maintain STAT3 nuclear accumulation. Similarly, it was described previously that the nerve growth factor–dependent transport of ERK5 from distal axons to the cell body and further translocation to the nucleus required endocytosis and microtubule transport (Ginty and Segal, 2002). For HGF/c-Met, the process would appear to be dynamic with constant dissociation and reassociation of STAT3 with activated c-Met endosomal complexes, with the steady-state phosphorylation being determined by the c-Met activity/phosphotyrosine phosphatase balance. This behavior would appear to be receptor specific because we show that oncostatin M–dependent nuclear uptake of STAT3 does not require receptor endocytosis and microtubule integrity. The kinase/phosphatase balance here is clearly different. Interestingly, HGF/c-Met–dependent ERK1/2 nuclear accumulation was not blocked by microtubule disruption (Fig. 3, G and H),

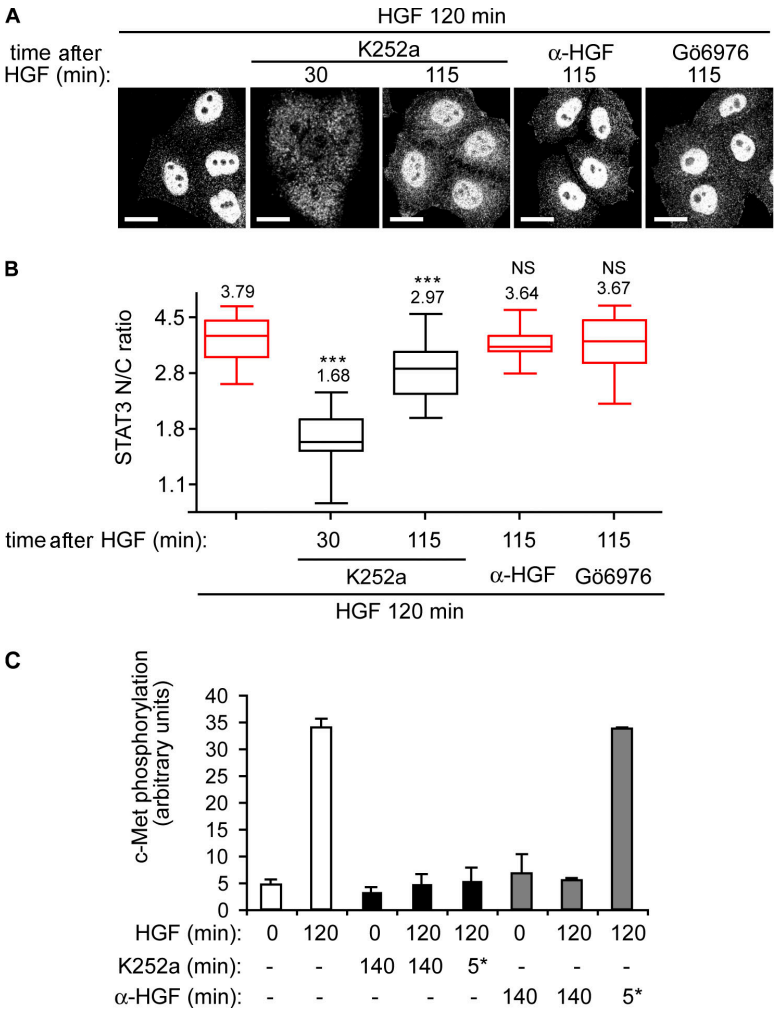

Figure 4. **STAT3 nuclear accumulation is controlled by c-Met activation in endosomal compartments.** (A) Confocal projections of cells stained for STAT3. Cells were stimulated for 120 min with HGF alone or in the presence of K252a or a neutralizing anti-HGF antibody or 1 µM Gö6976, added at 30 or 115 min, i.e., 90 or 5 min before fixation. Bars, 20 µm. (B) Quantitation of STAT3 nuclear-cytoplasmic ratios (STAT3 N/C ratio). ***, $P < 0.0002$. (C) Phospho–c-Met/tubulin ratios obtained by densitometric analysis of Western blots shown in Fig. S2 (I and J, available at http://www.jcb.org/cgi/content/full/jcb.200806076/DC1). Cells were stimulated with HGF for the times shown. 1 µM K252a or 30 µg/ml of a neutralizing HGF antibody was added for 0 or 140 min or for the final 5 min of HGF stimulation (5*). The graph represents the mean of two independent experiments. Error bars represent ranges.

which is indicative of both a functional endosomal c-Met and distinctive spatial constraints exerted on ERK1/2 activation. Consistent with this, microtubule disruption inhibited HGF-dependent STAT3 but not ERK1/2 phosphorylation (Fig. 3, I and J).

STAT3 nuclear accumulation upon HGF stimulation requires active endosomal c-Met

To asses whether maintenance of c-Met activity in endosomal compartments is necessary for HGF-dependent STAT3 nuclear accumulation, cells were treated with the inhibitor K252a, which has been previously shown to inhibit c-Met phosphorylation (Coltella et al., 2003). Cells were stimulated by HGF for 120 min alone or in the presence of K252a, added after 30 min or only for the last 5 min of this treatment, and STAT3 localization was analyzed by confocal microscopy (Fig. 4 A). The STAT3 nuclear-cytoplasmic ratio significantly decreased from 3.7 to 1.7 and 2.9 ($P < 0.0002$) upon addition of K252a at 30 and 115 min, respectively (Fig. 4, A and B). In contrast, when a neutralizing HGF antibody was added instead of K252a, the nuclear-cytoplasmic ratio was unchanged (Fig. 4, A and B), which is indicative of a lack of requirement for recycling and reactivation of the receptor. Preincubation with K252a or the neutralizing anti-HGF antibody before HGF stimulation for 15 or 120 min blocked c-Met phosphorylation. K252a addition after treatment (i.e., added for the last 5 min of a 120-min HGF stimulation) also inhibited c-Met phosphorylation (Fig. 4 C and Fig. S2 I). Addition after treatment with the neutralizing anti-HGF antibody had no effect (Fig. 4 C and Fig. S2 J). The effectiveness of acute exposure with the anti-HGF antibody was confirmed (Fig. S2 J). At 115 min of HGF treatment, c-Met had fully internalized and trafficked to the perinuclear compartment (Fig. 3 A, right, second from the top) and was not accessible to the neutralizing antibodies but remained accessible to the membrane-permeable inhibitor K252a. Similar results were obtained with the c-Met inhibitor SU-11274 (unpublished data). These results demonstrate that HGF-dependent STAT3 accumulation in the nucleus requires the retention of the c-Met perinuclear pool in an active state.

HGF triggers a weak STAT3 signal but a strong ERK1/2 signal

STAT3 pathway stimulation by HGF was further compared with oncostatin M stimulation to assess why distinct mechanisms might be required for signal delivery to the nucleus. STAT3 showed no significant increase in phosphorylation or nuclear accumulation on acute (15 and 30 min) HGF treatment. This is not a cell-specific idiosyncrasy because in the same model oncostatin M elicited strong responses (Fig. 5, A–C and E–I). This indicates

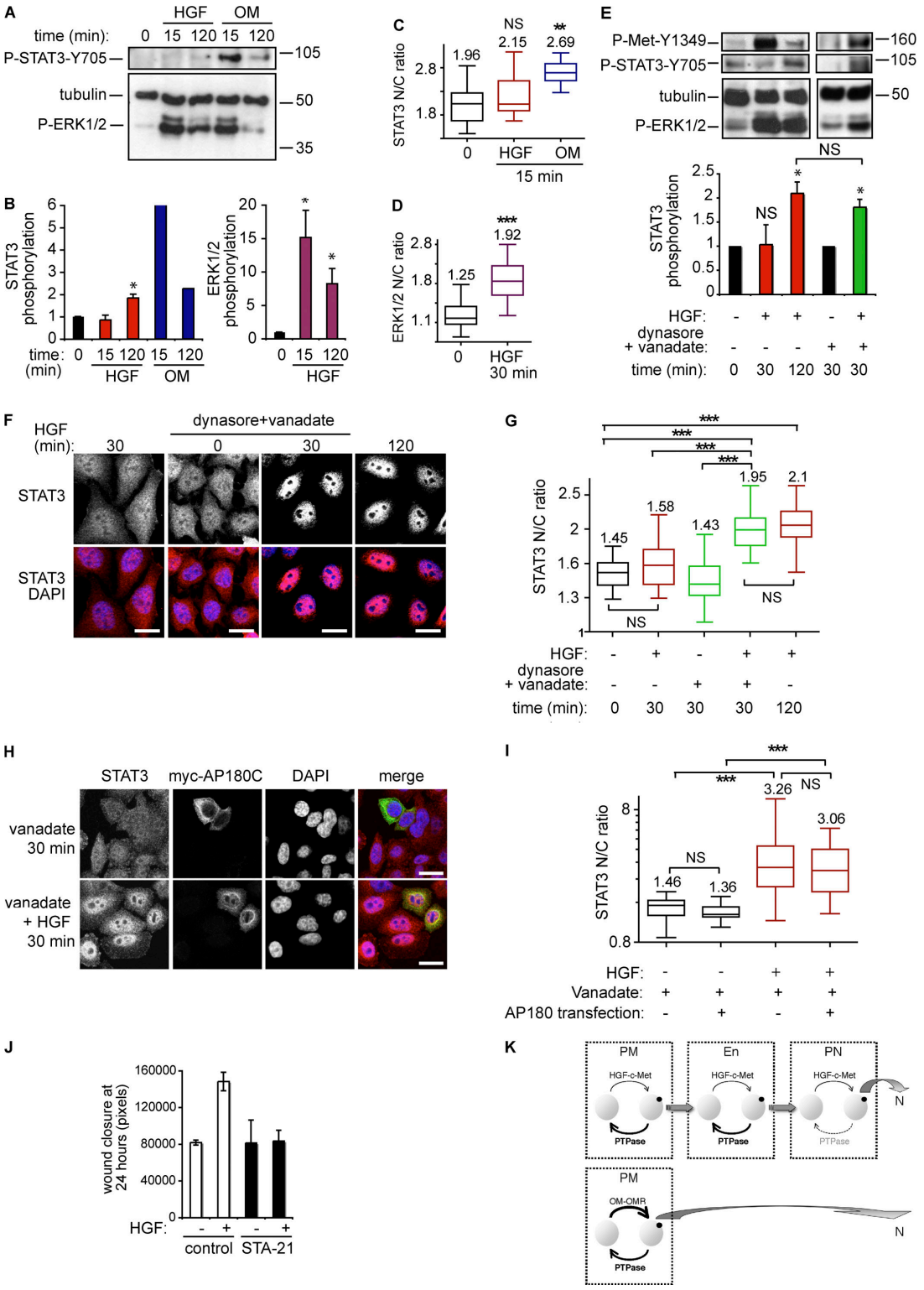

Figure 5. **HGF triggers a weak STAT3 signal but a strong ERK1/2 signal.** (A) HeLa cells were stimulated for 0, 15, or 120 min with HGF or oncostatin M. Western blot for P-STAT3 (Y705), tubulin, and P-ERK1/2. Molecular masses are shown in kD. (B) Densitometric analysis. The graphs represent the fold increases of P-STAT3/tubulin and P-ERK1/2/tubulin between stimulated and control and is the mean of three and two independent experiments for HGF and oncostatin M stimulation, respectively. Error bars represent SEM. (C) Quantitation of STAT3 nuclear-cytoplasmic ratios (STAT3 N/C ratio) at 0 and 15 min of stimulation with HGF or oncostatin M . **, $P < 0.001$ (pictures not shown). (D) Quantitation of ERK1/2 nuclear-cytoplasmic ratios at 0 and 30 min of stimulation with HGF. **, $P < 0.001$ (pictures not shown). (E) Cells were stimulated or not with HGF with or without 80 μM dynasore and 400 μM vanadate for the times indicated. Western Blot for P-c-Met (Y1349), P-STAT3 (Y705), tubulin, and P-ERK1/2. The graph represents P-STAT3/tubulin ratios obtained by densitometric analysis of three independent experiments. Molecular masses are shown in kD. *, $P < 0.05$. Error bars represent SEM. (F) Cells stimulated for the times indicated with HGF alone or in the presence of 80 μM dynasore and 400 μM vanadate were stained for STAT3 and DAPI. Confocal sections are shown. Bars, 20 μm. (G) Quantitation of STAT3 nuclear-cytoplasmic ratios. ***, $P < 0.0001$. (H) Confocal projections of five Z sections of cells with or without myc-AP180C and stained with STAT3, myc, and DAPI after 30 min of stimulation with vanadate alone (top) or with HGF (bottom). Bars, 20 μm.

that STAT3 can behave differently for distinct agonists. The delayed STAT3 response to HGF was signal specific because ERK1/2 showed a significant increase in phosphorylation under these conditions and nuclear accumulation of ERK1/2 was observed by 30 min of HGF stimulation (Fig. 5 D) when STAT3 was still absent (Fig. 5, A and B).

The different mechanisms of signal accumulation in the nucleus might reflect signal strength associated with distinct tyrosine kinase activation and phosphorylation of the signaling molecule. Thus, we hypothesized that despite the opposing action of phosphatases, the strength of STAT3 activation upon oncostatin M stimulation and of ERK1/2 activation on HGF stimulation are above a threshold that allows diffusion and nuclear uptake. By comparison, the activation of STAT3 in response to HGF is below the threshold set by phosphatases, and STAT3 is only effectively phosphorylated and accumulates in the nucleus upon delivery of activated c-Met to the perinuclear compartment, limiting exposure to STAT3 protein tyrosine phosphatases. Consistent with this, a 30-min treatment with HGF in the presence of the phosphatase inhibitor vanadate on cells pretreated with dynasore or concanavalin A triggered STAT3 phosphorylation and nuclear accumulation to a level comparable with 120 min of treatment with HGF alone (Fig. 5, E–G; and Fig. S3, A–D, available at http://www.jcb.org/cgi/content/full/jcb.200806076/DC1). Similar effects of vanadate were obtained in cells transfected with mycAP180C (Fig. 5, H and I) or pretreated with vinblastine (Fig. S3, E and F).

HGF-dependent wound healing of STAT3−/− keratinocytes has been shown to be impaired in vitro (Sano et al., 1999). To assess the STAT3 requirement in this study, wound healing experiments were performed. STAT3 localization was first analyzed in fixed HeLa cells at the leading edge of the wound. The nuclear-cytoplasmic ratio was increased significantly in migrating cells cultured in the presence of HGF as compared with the less motile cells cultured without HGF (Fig. S3, G and H). This suggested that STAT3 nuclear accumulation plays a role in HGF-dependent wound healing. It was found that HGF increased the wound closure of HeLa cells by twofold after 24 h (Fig. 5 J and Fig. S3 I). Incubation of cells with the recently described STAT3-selective inhibitor STA-21 (Song et al., 2005) blocked HGF-dependent wound closure. The inhibition was HGF specific and toxicity of the compound was excluded because, under basal conditions, STA-21 had no effect on wound healing (Fig. 5 J and Fig. S3 I). STA-21 has been reported to inhibit STAT3 nuclear translocation (Song et al., 2005) and this was verified in this study (Fig. S3 J). It can be surmised that HGF-dependent HeLa cell wound healing is dependent on the STAT3 pathway and specifically on STAT3 nuclear uptake driven by the endosomal traffic of c-Met.

This study shows that HGF-dependent STAT3 translocation to the nucleus requires c-Met delivery to the perinuclear compartment and is not triggered by plasma membrane phosphorylation and simple diffusion away from the activated c-Met. In contrast, oncostatin M, in the same cells, triggers nuclear accumulation of STAT3 independent of endocytosis. C-Met endocytosis is required for both ERK1/2 and STAT3 nuclear accumulation. However, although endocytosis alone is sufficient to support ERK1/2 nuclear accumulation, STAT3 accumulation requires microtubule traffic of c-Met to the perinuclear compartment. It is proposed that signal strength determines the nuclear proximity required for signal delivery. Thus, for a very strong signal as observed for oncostatin M–stimulated STAT3, sufficient phosphorylation occurs for an appropriate threshold to be reached permitting diffusion through a phosphatase-rich environment to reach and accumulate in the nucleus as a phosphoprotein. In contrast, it is proposed that the much weaker signal from c-Met to STAT3 requires the signal from the receptor itself to be juxtanuclear for the same threshold to be achieved, leading to STAT3 accumulation in the nucleus (Fig. 5 K, model). This is consistent not only with the requirement for endocytosis, but also for the subsequent traffic of the activated receptor to the perinuclear compartment to trigger/maintain an increase in nuclear STAT3. This insight into agonist action demonstrates that it is not simply the receptor and immediate adaptors and effectors that determine cellular responses but also the receptor location determined by the regulated traffic of the receptor. This traffic and the subsequent accumulation of nuclear STAT3 are evidently critical to HGF-induced migratory responses.

Materials and methods

Growth factor, antibodies, inhibitors and constructs

Purified human recombinant HGF was obtained from R&D Systems and oncostatin M from EMD. Transferrin conjugated to cy-3 was obtained from Jackson ImmunoResearch Laboratories. Alexa Fluor 555 Microscale Protein Labeling kit was used to label HGF according to the manufacturer's instructions. The following antibodies were used: goat polyclonal neutralizing anti-HGF (Sigma-Aldrich), goat polyclonal neutralizing anti–c-Met, monoclonal anti–human c-Met extracellular domain (clone DO24; Millipore), goat polyclonal anti-EEA1 (Santa Cruz Biotechnology, Inc.), and mouse monoclonal anti-tubulin (Sigma-Aldrich). Rabbit polyclonals used were the following: anti–phospho–c-Met (Tyrosine 1349 or Tyrosine 1234/1235), pan-ERK, phospho-p42/p44 ERK, mouse monoclonal anti–pan-STAT3, phospho-STAT3 (Y706; S727), PKCα (BD Biosciences), anti–pan-STAT3, and chc (Santa Cruz Biotechnologies, Inc.). The secondary antibodies used for Western blot were peroxidase-labeled monkey anti–mouse or anti–rabbit IgG (GE Healthcare). The secondary antibodies used for immunofluorescence experiments were Alexa 488–conjugated goat anti–rabbit IgG (Invitrogen), cy3-conjugated affinity-purified donkey anti–mouse IgG, and cy5-conjugated affinity-purified donkey anti–goat IgG (Jackson ImmunoResearch Laboratories). Gö6976 and vinblastine sulfate were obtained from EMD. K252a was obtained from Invitrogen. Vanadate, concanavalin A, and dynasore were obtained from Sigma-Aldrich. The pCMV-Myc r-AP180 C terminus (residues 530 to 915; myc-AP180-C) construct was a gift from H. McMahon (Neurobiology Division, Laboratory of Molecular Biology, Cambridge, England, UK). The pCMV-myc-dynamitin construct was obtained from C.J. Echeverri (Cenix Bioscience GmbH, Dresden, Germany; Burkhardt et al., 1997).

(I) Quantitation of STAT3 nuclear-cytoplasmic ratios. ***, $P < 0.0001$. (J) Quantitation of wound closure. The graph is the mean of two independent experiments performed in duplicate. Error bars represent SD. (K) Model of c-Met and oncostatin M receptor stimulation of STAT3 nuclear accumulation. PM, plasma membrane; En, peripheral endosome; PN, perinuclear endosome; N, nucleus. At the perinuclear location, the proximity of c-Met with the nucleus protects STAT3 against phosphatase activity, allowing a significant increase in nuclear accumulation.

Cell culture and transfection

HeLa cells and mouse embryo PKCα knockout or wild-type fibroblasts were cultured in DME (Cancer Research UK) supplemented with 10% FBS (Sigma-Aldrich) and maintained at 37°C in an humidified 10% CO_2 atmosphere. The cells were seeded at 10^5 cells in 35-mm plates (for Western blot experiments) or at 5×10^4 cells per well on coverslips in 24-well plates (for immunocytochemistry) and serum starved for 24 h. Before the stimulations, cells were incubated at 4°C for 10 min, and for a further 50 min in the presence or not of 100 ng/ml HGF or 10 ng/ml oncostatin M. Cells were then incubated at 37°C for various times from 0 to 120 min before fixation for immunofluorescence or harvesting for Western blots. Where indicated, the cells were preincubated with appropriate inhibitors 10 or 15 min before HGF stimulation and the inhibitors were maintained during subsequent stimulation. Preincubation with dynasore was for 30 min. Vanadate was added at the same time as HGF. Transfections were performed on subconfluent cells seeded in 24-well plates. For each well, 0.8 µg DNA was mixed with 1 µl Lipofectamine 2000 (Invitrogen) in 100 µl OPTIMEM1 with GlutaMAX (Gibco), incubated at room temperature for 20 min to allow the precipitate to form and directly added to the cells in their culture medium. 5 h later, the culture medium was changed. Stimulations were performed 24 h after transfection.

Immunofluorescence and confocal microscopy

HeLa cells were grown on coverslips, treated as described in the previous section, washed in PBS, and fixed in 2% PFA for 10 min. Free aldehydes were quenched with 50 mM NH_4Cl in PBS for 10 min. Fixed cells were permeabilized in 0.2% Triton X-100 in PBS/2% BSA for 15 min and then incubated at room temperature for 30 min with the primary antibodies. Cells were rinsed and incubated with appropriate secondary antibodies for 30 min. Cells were washed three times in PBS and once in water and then mounted in DAPI-containing mounting medium (BD Biosciences). All images were acquired using a confocal laser scanning microscope (LSM510; Carl Zeiss, Inc.) equipped with a 63×/1.4 NA Plan-Apochromat oil immersion objective. Alexa 488 was excited with the 488-nm line of an Argon laser, Cy3 was excited with a 543-nm HeNe laser, and Cy5 was excited with a 633-nm HeNe laser.

Statistical analysis of confocal images

For quantitation of STAT3 nucleocytoplasmic ratios, double staining of STAT3 and DAPI was performed. Confocal Z-stacks of five sections each of 0.8 µm from the base to the apex of cells were acquired randomly and projected in one picture, which was analyzed using Photoshop CS2 (Adobe). STAT3 mean intensity was measured in the cytoplasm and in the nucleus as defined by DAPI staining. Nucleocytoplasmic ratios were then obtained. For each condition in each experiment, at least 15 cells were analyzed. Data from at least three experiments for each condition were pooled and analyzed statistically. We used a nonparametric Mann-Whitney test to compare medians using InStat software (version 3.0 for Mac 2001; GraphPad Software, Inc.). To interpret the distribution of data, box and whisker plots were used. The box and whisker plot is a histogram-like method for displaying upper and lower quartiles and maximum and minimum values in addition to median. The scale is in log10 and the mean value is indicated on top of each box. Plots represent the results of three independent experiments.

Western blot analysis

Cells cultured in 6-well plates were harvested in 150 µl of sample buffer (Invitrogen) and boiled for 10 min. Samples were loaded on 4–12% gradient polyacrylamide gels (Invitrogen). Separated proteins were transferred to a 0.45-µm nitrocellulose transfer membrane (Whatman). Protein loading was checked by staining with Ponceau Red. Membranes were then blotted with appropriate first antibodies at a dilution of 1:1,000. Specific binding of antibodies was detected with appropriate peroxidase-conjugated secondary antibodies and visualized by enhanced chemiluminescence detection (GE Healthcare). Densitometric analyses of immunoblots were performed using ImageJ 1.36b (National Institutes of Health). Each value, indicated as a fold increase, corresponds to the mean of three independent experiments.

RNAi

The following 21-mer oligoribonucleotide pairs were obtained from QIAGEN: control, 50-UUCUCCGAACGUGUCACGUTT-30 and 50-ACGUGACACGUUCGGAGAATT-30; CHC, 50-GAAGGCUCGAGAGUCCUAUTT-30 and 50-AUAGGACUCUCGAGCCUUCTT-30; and PKCα, 50-GGCUUCCAGUGCCAAGUUUTT-30 and 50-AAACUUGGCACUGGAAGCCTT-30. The uniqueness of each RNAi recognition sequence was confirmed by blasting against GenBank database. The RNAi control does not match any known sequence. Cells were plated at 10^5 per well or 5×10^4 per well in six-well or 24-well plates, respectively. They were transfected the next day in medium without serum using oligofectamine (Invitrogen) with 10 or 2 µl of 20 µM RNAi and 5 or 1 µl of transfection reagent per well for 6- and 24-well plates, respectively. 10% of serum was added 4 h later. The cells were stimulated and harvested after 72 h.

Wound-healing assays

Confluent cells, deprived for 24 h in 0.5% FBS, were wounded with a pipette tip to obtain one or two perpendicular wounds in each well. The cultures were rinsed once and fresh medium was added with or without HGF and with or without drugs as indicated in figure legends. Images were acquired on a microscope (Axiovert TM 135; Carl Zeiss, Inc.) equipped with a 5 objective lens and a charge-coupled device camera (Orca ER; Hamamatsu Photonics) using Acquisition Manager (Kinetic Imaging) in the same area of each wound at time 0 and 24 h. For each picture, cell areas were measured as pixels using Photoshop CS2 (Adobe), and wound closure was calculated by subtracting the cell area at 24 h from the cell area at 0 h for each wound.

Online supplemental material

Fig. S1 shows STAT3 and P-STAT3 nuclear accumulation upon HGF stimulation and controls/quantitations for the c-Met endocytosis block. Fig. S2 shows the effect of concanavalin A on STAT3 nuclear accumulation and phosphorylation, tubulin cytoskeleton disruption under vinblastine treatment, lack of STAT3 nuclear accumulation in myc-dynamitin–transfected cells, decrease of STAT3 nuclear uptake in cells knocked down for PKCα and effects of K252a or a neutralizing anti-HGF antibody on c-Met phosphorylation. Fig. S3 shows the effect of vanadate on HGF-dependent STAT3 phosphorylation and nuclear accumulation when c-Met is maintained at the plasma membrane or in the endosome (upon concanavalin A or vinblastine treatment, respectively) and implication of STAT3 pathway in HGF-dependent wound healing. Online supplemental material is available at http://www.jcb.org/cgi/content/full/jcb.200806076/DC1.

We thank Sharon Tooze and Giampietro Schiavo for critical reading of the paper, Simone Radlke for helpful discussions, and Carine Joffre for the HGF labeling.

This work was funded by Cancer Research UK and the Medical Research Council.

Submitted: 12 June 2008
Accepted: 7 August 2008

References

Bild, A.H., J. Turkson, and R. Jove. 2002. Cytoplasmic transport of Stat3 by receptor-mediated endocytosis. *EMBO J.* 21:3255–3263.

Birchmeier, C., W. Birchmeier, E. Gherardi, and G.F. Vande Woude. 2003. Met, metastasis, motility and more. *Nat. Rev. Mol. Cell Biol.* 4:915–925.

Boccaccio, C., M. Ando, L. Tamagnone, A. Bardelli, P. Michieli, C. Battistini, and P.M. Comoglio. 1998. Induction of epithelial tubules by growth factor HGF depends on the STAT pathway. *Nature.* 391:285–288.

Burkhardt, J.K., C.J. Echeverri, T. Nilsson, and R.B. Vallee. 1997. Overexpression of the dynamitin (p50) subunit of the dynactin complex disrupts dynein-dependent maintenance of membrane organelle distribution. *J. Cell Biol.* 139:469–484.

Christensen, J.G., J. Burrows, and R. Salgia. 2005. c-Met as a target for human cancer and characterization of inhibitors for therapeutic intervention. *Cancer Lett.* 225:1–26.

Coltella, N., M.C. Manara, V. Cerisano, L. Trusolino, M.F. Di Renzo, K. Scotlandi, and R. Ferracini. 2003. Role of the MET/HGF receptor in proliferation and invasive behavior of osteosarcoma. *FASEB J.* 17:1162–1164.

Cramer, A., S. Kleiner, M. Westermann, A. Meissner, A. Lange, and K. Friedrich. 2005. Activation of the c-Met receptor complex in fibroblasts drives invasive cell behavior by signaling through transcription factor STAT3. *J. Cell. Biochem.* 95:805–816.

Ginty, D.D., and R.A. Segal. 2002. Retrograde neurotrophin signaling: Trk-ing along the axon. *Curr. Opin. Neurobiol.* 12:268–274.

Graveel, C.R., C.A. London, and G.F. Vande Woude. 2005. A mouse model of activating met mutations. *Cell Cycle.* 4:518–520.

Heinrich, P.C., I. Behrmann, S. Haan, H.M. Hermanns, G. Muller-Newen, and F. Schaper. 2003. Principles of interleukin (IL)-6-type cytokine signalling and its regulation. *Biochem. J.* 374:1–20.

Howe, C.L. 2005. Modeling the signaling endosome hypothesis: why a drive to the nucleus is better than a (random) walk. *Theor. Biol. Med. Model.* 2:43.

Kermorgant, S., and P.J. Parker. 2005. c-Met signalling: spatio-temporal decisions. *Cell Cycle.* 4:352–355.

Kermorgant, S., D. Zicha, and P.J. Parker. 2003. Protein kinase C controls microtubule-based traffic but not proteasomal degradation of c-Met. *J. Biol. Chem.* 278:28921–28929.

Kermorgant, S., D. Zicha, and P.J. Parker. 2004. PKC controls HGF-dependent c-Met traffic, signalling and cell migration. *EMBO J.* 23:3721–3734.

Kholodenko, B.N. 2006. Cell-signalling dynamics in time and space. *Nat. Rev. Mol. Cell Biol.* 7:165–176.

Liu, L., K.M. McBride, and N.C. Reich. 2005. STAT3 nuclear import is independent of tyrosine phosphorylation and mediated by importin-alpha3. *Proc. Natl. Acad. Sci. USA.* 102:8150–8155.

Macia, E., M. Ehrlich, R. Massol, E. Boucrot, C. Brunner, and T. Kirchhausen. 2006. Dynasore, a cell-permeable inhibitor of dynamin. *Dev. Cell.* 10:839–850.

Miaczynska, M., L. Pelkmans, and M. Zerial. 2004. Not just a sink: endosomes in control of signal transduction. *Curr. Opin. Cell Biol.* 16:400–406.

Polo, S., and P.P. Di Fiore. 2006. Endocytosis conducts the cell signaling orchestra. *Cell.* 124:897–900.

Pranada, A.L., S. Metz, A. Herrmann, P.C. Heinrich, and G. Muller-Newen. 2004. Real time analysis of STAT3 nucleocytoplasmic shuttling. *J. Biol. Chem.* 279:15114–15123.

Reich, N.C., and L. Liu. 2006. Tracking STAT nuclear traffic. *Nat. Rev. Immunol.* 6:602–612.

Sano, S., S. Itami, K. Takeda, M. Tarutani, Y. Yamaguchi, H. Miura, K. Yoshikawa, S. Akira, and J. Takeda. 1999. Keratinocyte-specific ablation of Stat3 exhibits impaired skin remodeling, but does not affect skin morphogenesis. *EMBO J.* 18:4657–4668.

Schenck, A., L. Goto-Silva, C. Collinet, M. Rhinn, A. Giner, B. Habermann, M. Brand, and M. Zerial. 2008. The endosomal protein Appl1 mediates Akt substrate specificity and cell survival in vertebrate development. *Cell.* 133:486–497.

Shah, M., K. Patel, S. Mukhopadhyay, F. Xu, G. Guo, and P.B. Sehgal. 2006. Membrane-associated STAT3 and PY-STAT3 in the cytoplasm. *J. Biol. Chem.* 281:7302–7308.

Song, H., R. Wang, S. Wang, and J. Lin. 2005. A low-molecular-weight compound discovered through virtual database screening inhibits Stat3 function in breast cancer cells. *Proc. Natl. Acad. Sci. USA.* 102:4700–4705.

Trusolino, L., and P.M. Comoglio. 2002. Scatter-factor and semaphorin receptors: cell signalling for invasive growth. *Nat. Rev. Cancer.* 2:289–300.

Zhang, Y.W., L.M. Wang, R. Jove, and G.F. Vande Woude. 2002. Requirement of Stat3 signaling for HGF/SF-Met mediated tumorigenesis. *Oncogene.* 21:217–226.